2021 43rd Annual International Conference of the
IEEE Engineering in Medicine & Biology Society (EMBC)
Oct 31 - Nov 4, 2021. Virtual Conference

Magnetic-free Extended Kalman Filter for upper limb kinematic assessment in Yoga

L. Truppa, P. Garofalo, M. Raggi, E. Bergamini, G. Vannozzi, A. M. Sabatini, and A. Mannini

Abstract— **Human motion analysis is gaining increased importance in several fields, from movement assessment in rehabilitation to recreational applications such as virtual coaching. Among all the technologies involved in motion capture, Magneto-Inertial Measurements Units (MIMUs) is one of the most promising due to their small dimensions and low costs. Nevertheless, their usage is strongly limited by different error sources, among which magnetic disturbances, which are particularly problematic in indoor environments. Inertial Measurement Units (IMUs) could, thus, be considered as alternative solution. Indeed, relying exclusively on accelerometers and gyroscopes, they are insensitive to magnetic disturbances. Even if the literature has started to propose few algorithms that do not take into account magnetometer input, their application is limited to robotics and aviation. The aim of the present work is to introduce a magnetic-free quaternion based Extended Kalman filter for upper limb kinematic assessment in human motion (*i.e.*, yoga). The algorithm was tested on five expert yoga trainers during the execution of the sun salutation sequence. Joint angle estimations were compared with the ones obtained from an optoelectronic reference system by evaluating the Mean Absolute Errors (MAEs) and Pearson's correlation coefficients. The achieved worst-case was 6.17°, while the best one was 2.65° for MAEs mean values. The accuracy of the algorithm was further confirmed by the high values of the Pearson's correlation coefficients (lowest mean value of 0.86).**

Clinical Relevance— **The proposed work validated a magnetic free algorithm for kinematic reconstruction with inertial units. It could be used as a wearable solution to track human movements in indoor environments being insensitive to magnetic disturbances, and thus could be potentially used also for rehabilitation purposes.**

I. Introduction

Human movement analysis aims at gathering quantitative information about the mechanics of the musculo-skeletal system during the execution of a motor task. Nowadays, different technologies are used to carry out human motion analysis, such as infrared optoelectronic systems (OMCs) [1], Magneto-Inertial Measurement Units (MIMU) [2] and video camera based systems [3]. Among them, the "gold standard" for motion tracking are OMCs, which are based on the triangulation on several retro-reflective markers attached to the body [4]. Although these systems are characterized by high accuracies, they require a controlled environment and specific skills to be used, turning out to be impractical with outdoor applications. On the other hand, MIMUs result extremely user-friendly, cheap and small-in-size sensors. They can be used in uncontrolled environments too, but they are less accurate for kinematic estimation compared to OMCs. MIMUs are multi-sensor platforms composed by triaxial accelerometer, gyroscope and magnetometer. The algorithms, used to obtain orientation information from MIMUs, are generally referred to as "*sensor fusion*" algorithms and they exploit the data from multiple sensors to give a reliable estimation of kinematic parameters, such as joint angles. Among them, Kalman filters are considered among the most reliable, efficient and robust sensor fusion algorithm [5]. In particular, attitude estimation is a classic non-linear problem so the Extended Kalman Filter is generally used [6]. As concerns MIMUs, attitude estimation is influenced by magnetic disturbances (*i.e.*, presence of ferromagnetic object). This phenomenon greatly limits the indoor applications of MIMU technology [7]. On the other hand, Inertial Measurement Units (IMUs), composed by accelerometers and gyroscopes only, represent an alternative technology to MIMUs being insensitive to magnetic disturbances. Several solutions have been introduced to estimate the orientation from inertial sensors. Complementary filters [8] estimates the attitude using gyroscopes and accelerometers data only. They showed good capabilities but they did not rely on a model for describing the process, which could cause a loss of accuracy [9]. Instead, extended and unscented Kalman filters are characterized by higher estimation precision because of the presence of a process model that could fix observational data. Nevertheless, only few studies exploited gyroscopes and accelerometers exclusively and their application was limited to robotics [10] and aviation.

Based on this, the purpose of this study is to validate a magnetic-free algorithm for human kinematic reconstruction to be used in indoor environments, in which the presence of ferromagnetic objects could significantly reduce the quality of the recordings. To this aim, we developed an Extended Kalman Filter based on IMUs and we tested it in an indoor sport application, tracking upper limb motion during a yoga sequence of poses. In our knowledge, no previous study has applied an Extended Kalman Filter for kinematic assessment

L. Truppa (corresponding author, e-mail: luigi.truppa@santannapisa.it, number: +39 3886549865) and A.M. Sabatini (e-mail: angelo.sabatini@santannapisa.it) are with the Biorobotics Institute and the Department of Excellence in Robotics & AI, (Scuola Superiore Sant'Anna, Pisa, Italy.

P. Garofalo (e-mail: pietro.garofalo@turingsense.com) and M. Raggi (michele.raggi@turingsense.com) are with TuringSense EU lab (Forlì, Italy).

A. Mannini (e-mail: andrea.mannini@santannapisa.it) is with the Biorobotics Institute and the Department of Excellence in Robotics & AI (Scuola Superiore Sant'Anna, Pisa, Italy) and with IRCCS Fondazione Don Carlo Gnocchi (Firenze, Italy)

E. Bergamini (e-mail elena.bergamini@uniroma4.it) and G. Vannozzi (e-mail: giuseppe.vannozzi@uniroma4.it) are with Università degli Studi "Foro Italico" (Roma, Italy)

in peculiar movements such as the ones introduced by the proposed yoga sequence. This physical activity involves complex full body postures in which the upper limb pose changes significantly, exploring a very large range of motion. We choose an Extended Kalman filter which follows the same rules of the classic linear Kalman Filter through the linearization of the non-linear process. The joint angles estimated with IMUs were compared with the one calculated using an optoelectronic system to assess the correctness of the estimations.

II. Materials and Methods

A. Participants

Five expert yoga practitioners (age: 24.0±3.3 years, height: 180.8±6.3 cm, mass: 72.4±8.3 kg) were involved in tests. Participants, in accordance with the Helsinki protocol, signed an informed consent form to take part to the study.

B. Experimental procedure

Four IMUs (TuringSense, Santa Clara, US, sampling rate: 100 Hz) were placed laterally on the right upper limb and on the trunk using elastic bands. Each IMU was mounted on a 3D-printed plastic support together with three reflective markers needed to acquire reference data from the OMC. After the preliminary placement of the IMUs, participants performed the sun salutation sequence in a controlled environment (*i.e.*, laboratory of biomechanics).

C. Biomechanical model

For each segment involved in the study (*i.e.*, trunk – TRK, right upper arm – RUA, right lower arm – RLA and right hand – RHD) an anatomical frame was defined from both OMC and IMU data. The abovementioned reference frame was built by matching the *y*-axis (*i.e.*, internal-external rotation axis) with the longitudinal axis of the right upper limb segments, the *x*-axis (*i.e.*, flexion-extension axis) coming out laterally from left to right and the *z*-axis (*i.e.*, abduction-adduction axis) orthogonal to the others (out of the plane). In the attempt of avoiding the use of the magnetometer, one of the usually adopted reference directions in the global frame, that is the Earth magnetic field direction, becomes unavailable. This calls for the need of a new reference vector that can be obtained from anatomical considerations by asking the participant to execute a functional movement wearing sensors before the experiment itself. We adopted the approach previously proposed by Ligorio et al. [11]. Indeed, the flexion-extension direction as measured by the gyroscopes during a preliminary functional movement can be used to define a horizontal vector ($\boldsymbol{e}_{1s}$, in which the angular velocity vector during the flexion is used - $\bar{\boldsymbol{\omega}}|_{flexion}$) in the orthogonal plane with respect to the gravity vector. Thus, the first axis of the sensor frame was the gravity vector ($\boldsymbol{e}_{2s}$ that exploited the acceleration measured by the accelerometers during the N-pose - $\bar{\boldsymbol{a}}|_{Npose}$) measured by accelerometers during a preliminary N-pose (static position with the arm relaxed along the body), the second one was $\boldsymbol{e}_{1s}$ and the third one was the cross product between them.

Body reference frame:

$$\boldsymbol{e}_{1a} = \begin{bmatrix}1\\0\\0\end{bmatrix}, \boldsymbol{e}_{2a} = \begin{bmatrix}0\\1\\0\end{bmatrix}, \boldsymbol{e}_{3a} = \begin{bmatrix}0\\0\\1\end{bmatrix} \quad (1)$$

Sensor reference frame:

$$\boldsymbol{e}_{1s} = \frac{\bar{\boldsymbol{\omega}}|_{flexion}}{\left\|\bar{\boldsymbol{\omega}}|_{flexion}\right\|} - \frac{\left(\frac{\bar{\boldsymbol{\omega}}|_{flexion}}{\left\|\bar{\boldsymbol{\omega}}|_{flexion}\right\|} \bullet \boldsymbol{e}_{2s}\right)}{\|\boldsymbol{e}_{2s}\|^2}\boldsymbol{e}_{2s}$$
$$\boldsymbol{e}_{2s} = \frac{\bar{\boldsymbol{a}}|_{Npose}}{\left\|\bar{\boldsymbol{a}}|_{Npose}\right\|} \quad (2)$$
$$\boldsymbol{e}_{3s} = \frac{\boldsymbol{e}_{1s} \times \boldsymbol{e}_{2s}}{\|\boldsymbol{e}_{1s} \times \boldsymbol{e}_{2s}\|}$$

The cosine matrix that describes the rotation from the sensor frame to the anatomical one was estimated as follows:

$$R_a^s = [\boldsymbol{e}_{1a} \quad \boldsymbol{e}_{2a} \quad \boldsymbol{e}_{3a}][\boldsymbol{e}_{1s} \quad \boldsymbol{e}_{2s} \quad \boldsymbol{e}_{3s}]^{-1} \quad (3)$$

From $\boldsymbol{R}_a^s$ the corresponding quaternion $\boldsymbol{q}_a^s$ was calculated.

D. Extended Kalman Filter

Since attitude estimation is a classic example of a non-linear problem, a classic Extended Kalman Filter was used [6]. Considering the relative high sampling rate (i.e., 100 Hz), the time-discrete version of the Extended Kalman Filter is here used. As mentioned above, the algorithm relies on the gyroscopes ($\boldsymbol{\omega}$) and accelerometers ($\boldsymbol{a}$) signals only, which can be modeled as follows:

$$\begin{cases} \boldsymbol{a} = K_a(\boldsymbol{g} + \boldsymbol{a}_{inertial}) + \boldsymbol{b}_a + \boldsymbol{v}_a \\ \boldsymbol{\omega} = K_g\boldsymbol{\omega}_{\boldsymbol{inertial}} + \boldsymbol{b}_{\boldsymbol{g}} + \boldsymbol{v}_{\boldsymbol{g}} \end{cases} \quad (4)$$

Where K_a and K_g are the scale factor matrix, which we assumed to be the identity matrix (*i.e.*, ideal case), $\boldsymbol{b}_a$ and $\boldsymbol{b}_{\boldsymbol{g}}$ are the accelerometers and gyroscopes bias respectively that were assumed to be null because before each acquisition a sensor calibration was done. Vectors $\boldsymbol{v}_a$ and $\boldsymbol{v}_{\boldsymbol{g}}$ are white noise with zero mean and covariance matrices Σ_a and Σ_g:

$$\Sigma_a = \begin{bmatrix}\sigma_{a_x}^2 & 0 & 0\\ 0 & \sigma_{a_y}^2 & 0\\ 0 & 0 & \sigma_{a_z}^2\end{bmatrix}, \Sigma_g = \begin{bmatrix}\sigma_{g_x}^2 & 0 & 0\\ 0 & \sigma_{g_y}^2 & 0\\ 0 & 0 & \sigma_{g_z}^2\end{bmatrix} \quad (5)$$

The state vector of the proposed filter is composed by the orientation quaternion only (in this paper the convention with the scalar part of the quaternion placed at the fourth element is used [12]).

$$\boldsymbol{x}_k = \boldsymbol{q}_k = \begin{bmatrix}\bar{q}\\ q_4\end{bmatrix} = \begin{bmatrix}q_1\\ q_2\\ q_3\\ q_4\end{bmatrix} \quad (6)$$

Equation (7) and Equation (8) shows the state transition equation and the measurement model respectively.

$$\boldsymbol{x}_{k+1} = A_k\boldsymbol{x}_k + \boldsymbol{v}_{x_k} \quad (7)$$

$$\boldsymbol{z}_{k+1} = f(\boldsymbol{x}_{k+1}) + \boldsymbol{v}_{k+1} = \begin{bmatrix}C(\boldsymbol{x}_{k+1})\boldsymbol{a}_0\\ C(\boldsymbol{x}_{k+1})\boldsymbol{h}_0\end{bmatrix} + \begin{bmatrix}\boldsymbol{v}_a\\ \boldsymbol{v}_{\boldsymbol{g}}\end{bmatrix} \quad (8)$$

where A_k is defined as in Equation (9) and $\boldsymbol{v}_{x_k}$ is the process noise, which is strictly connected to the gyroscope noise [6]:

$$A_k = I_{3x3}\cos(0.5\|\boldsymbol{\omega}_{\boldsymbol{k}}\|T_s) + \begin{bmatrix}[\boldsymbol{\omega}_{\boldsymbol{k}}]_\times & \boldsymbol{\omega}_{\boldsymbol{k}}\\ -\boldsymbol{\omega}_{\boldsymbol{k}}^T & 0\end{bmatrix}\frac{\sin(0.5\|\boldsymbol{\omega}_{\boldsymbol{k}}\|T_s)}{\|\boldsymbol{\omega}_{\boldsymbol{k}}\|} \quad (9)$$

$$\boldsymbol{v}_{x_k} = -\frac{T_s}{2}\begin{bmatrix}[\overline{q_k}]_\times + q_{4_k} I_{3x3} \\ -\overline{q_k}^T\end{bmatrix}\boldsymbol{v_g} \quad (10)$$

T_s is the sample rate. As concerns the measurements model, $C(\boldsymbol{x}_{k+1})$, $\boldsymbol{a_0}$ and $\boldsymbol{h_0}$ are defined by Equations (20) and (22) respectively, while $\boldsymbol{v}_a$ and $\boldsymbol{v_g}$ are white noise with zero mean and covariance matrices defined by Equation (5).

Prediction step

$$\boldsymbol{x}_{k+1}^- = A_k \boldsymbol{x}_k \quad (11)$$

$$P_{k+1}^- = A_k P_k A_k^T + Q_k \quad (12)$$

Where $\boldsymbol{x}_{k+1}^-$ is the *a priori* state, P_{k+1}^- is the *a priori* error covariance matrix. Q_k is the process noise covariance, which is directly linked to the gyroscope noise covariance matrix, since the quaternion is propagated using only the angular velocities.

$$Q_k = \left(\frac{T_s}{2}\right)^2 G_k \Sigma_g G_k^T \quad (13)$$

where G_k is [6]:

$$G_k = \begin{bmatrix}[\overline{x_k}]_\times + x_{4_k} I_{3x3} \\ -\overline{x_k}^T\end{bmatrix} \quad (14)$$

Filtering step

$$z_{pred} = \begin{bmatrix} C(\boldsymbol{x}_{k+1}^-)\boldsymbol{a}_0 \\ C(\boldsymbol{x}_{k+1}^-)\boldsymbol{h}_0 \end{bmatrix} \quad (15)$$

$$K_{k+1} = P_{k+1}^- \nabla z_{pred}^T (\nabla z_{pred} P_{k+1}^- \nabla z_{pred}^T + D) \quad (16)$$

$$\boldsymbol{x}_{k+1} = \boldsymbol{x}_{k+1}^- + K_{k+1}(\begin{bmatrix}\boldsymbol{a}_{k+1} \\ \boldsymbol{h}_{k+1}\end{bmatrix} - z_{pred}) \quad (17)$$

$$P_{k+1} = (I_{4x4} - K \nabla z_{pred})\, P_{k+1}^- \quad (18)$$

Where K_{k+1} is the filter gain, $\boldsymbol{x}_{k+1}$ and P_{k+1} the *a posteriori* state and error covariance matrix, while $C(\boldsymbol{x}_{k+1}^-)$ is defined as in (20) and D as:

$$D = \begin{bmatrix}\Sigma_a & 0 \\ 0 & \Sigma_g\end{bmatrix} \quad (19)$$

with:

$$s = \|\boldsymbol{x}\|^2 = x_1^2 + x_2^2 + x_3^2 + x_4^2 \quad (21)$$

In addition, we assumed that:

$$\boldsymbol{h}_0 = \boldsymbol{e}_{1s}, \qquad \boldsymbol{a}_0 = \boldsymbol{e}_{2s} \quad (22)$$

$$\boldsymbol{h}_{k+1} = e^{(-[\boldsymbol{\omega_k}]_\times T_s)} \boldsymbol{h}_k \quad (23)$$

E. Joint angles estimation

Joint cardan angles were estimated from the corresponding joint quaternions [11] by exploiting equation (24), in which ds is the distal segment and *ps* is the proximal one. The symbol ⊗ represents the Hamiltonian product between quaternions.

$\boldsymbol{q}_{\boldsymbol{ntrunk}}^{\boldsymbol{nds}}/\boldsymbol{q}^{-\boldsymbol{1}}{}_{\boldsymbol{ntrunk}}^{\boldsymbol{nps}}$ are the quaternions that describe the misalignment between the global reference frame of the corresponding body segment and the trunk frame. Indeed, since the algorithm relied only on gyroscopes and accelerometers, each IMU is characterized by a different global reference frame. The trunk frame was thus considered as the reference to which realign the global frames of each IMU [11]:

$$q_{ntrunk}^{ns} = \boldsymbol{x}_{\boldsymbol{s}}^{-\boldsymbol{1}}|_{Npose} \otimes \boldsymbol{q}_{\boldsymbol{s}}^{-\boldsymbol{1}}{}_{\boldsymbol{a}}^{\boldsymbol{s}} \otimes \boldsymbol{q}_{\boldsymbol{trunk}}{}_{\boldsymbol{a}}^{\boldsymbol{s}} \otimes \boldsymbol{x}_{\boldsymbol{trunk}}|_{Npose} \quad (25)$$

E. Data analysis

In order to verify the accuracy of yoga joint angles estimation, the joint error quaternions between OMC and IMU were computed as follows [13]:

$$\Delta q = (\boldsymbol{q}_{IMU})^{-1} \otimes (\boldsymbol{q}_{OMC}) \quad (26)$$

Therefore, the error joint angles ($\Delta\alpha_x, \Delta\alpha_y, \Delta\alpha_z$) were estimated from Δq. The Mean Absolute Error (MAE) was calculated as follows:

$$MAE_{x,y,z} = \frac{\sum_{k=1}^{N} \left|\Delta\alpha_{x,y,z_k}\right|}{N} \quad (27)$$

In addition, Pearson's correlation coefficients between IMU and OMC were estimated for each angle.

III. Results

A graphical representation of the estimated joint angles is reported in Figure 1. Finally, MAEs and Pearson's correlation coefficient values are shown in Table 1.

TABLE I. MAEs (mean ± standard deviation) and Pearson's correlation coefficients

	AB/AD	IR/ER	FE
Wrist			
MAE [°]	4.80 ± 0.70	4.45 ± 1.81	6.17 ± 0.87
Pearson	0.86 ± 0.16	0.88 ± 0.12	0.99 ± 0.01
Elbow			
MAE [°]	3.28 ± 2.00	3.24 ± 0.77	2.65 ± 1.28
Pearson	0.94 ± 0.04	0.96 ± 0.01	0.88 ± 0.11
Shoulder			
MAE [°]	4.45 ± 1.87	3.16 ± 0.95	4.54 ± 2.16
Pearson	0.98 ± 0.02	0.98 ± 0.02	0.99 ± 0.01

IV. Discussions

The present work introduced a magnetic-free quaternion

$$C(\boldsymbol{x}) = \frac{1}{s}\begin{bmatrix} x_1^2 - x_2^2 - x_3^2 + x_4^2 & 2(x_1x_2 + x_3x_4) & 2(x_1x_3 - x_2x_4) \\ 2(x_1x_2 - x_3x_4) & x_4^2 + x_2^2 - x_3^2 - x_1^2 & 2(x_2x_3 + x_1x_4) \\ 2(x_1x_3 + x_2x_4) & 2(x_2x_3 - x_1x_4) & x_3^2 + x_4^2 - x_1^2 - x_2^2 \end{bmatrix} \quad (20)$$

$$\boldsymbol{q}_{joint} = (\boldsymbol{q}_{\boldsymbol{ds}}{}_{\boldsymbol{a}}^{\boldsymbol{s}} \otimes \boldsymbol{x}|_{ds} \otimes \boldsymbol{q}_{\boldsymbol{ntrunk}}^{\boldsymbol{nds}}) \otimes (\boldsymbol{q}^{-\boldsymbol{1}}{}_{\boldsymbol{ntrunk}}^{\boldsymbol{nps}} \otimes \boldsymbol{x}^{-\boldsymbol{1}}|_{ps} \otimes \boldsymbol{q}_{\boldsymbol{ps}}{}_{\boldsymbol{a}}^{\boldsymbol{s}}) \quad (24)$$

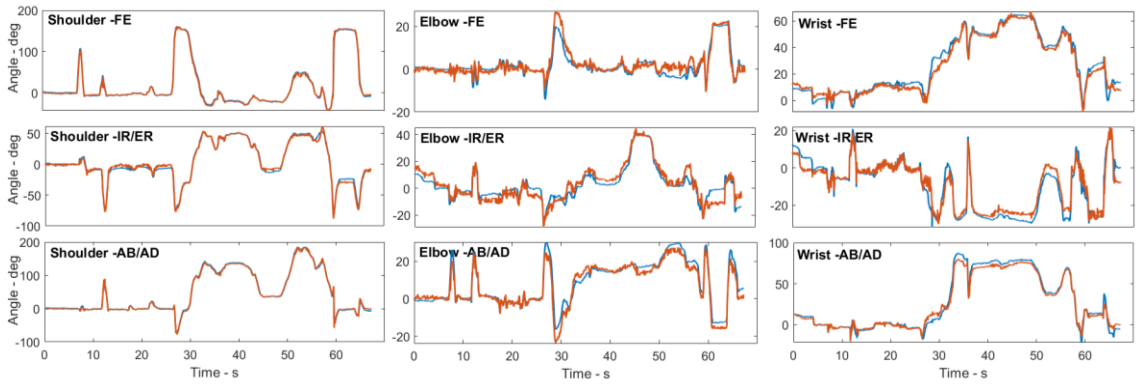

Figure 1: Example of IMU (in blue) and OMC (in orange) joint angles estimations

based Extended Kalman Filter for attitude estimation in human motion tracking applications. The filter was validated during Yoga poses on upper limb kinematics. It relies on gyroscopes and accelerometers only, making it insensitive to magnetic disturbances and thus particularly convenient in indoor applications, where magnetic disturbances and ferromagnetic objects may jeopardize the attitude estimation accuracy. The comparison between IMU and OMC showed an average MAE that ranges from 2.65° to 6.17° for the flexion-extension angle. Considering the small errors observed despite the large range of motion of the right upper limb during the sun salutation sequence (up to 200 degrees), the proposed solution seems suitable for motion tracking in uncontrolled environments. Indeed, alternative solutions considering also the magnetometer shows similar performances in using the Earth magnetic field as second reference vector. As example, Sabatini [6] developed an Extended Kalman filter using also the magnetometer information, obtaining an overall accuracy of 4.57 ° (1.31° for the roll angle, 1.40° for pitch angle and 4.13 for yaw angle), while Yun et al. [14] developed a Kalman filter for human motion tracking with an accuracy that ranged from 2° to 9°, depending on the velocity of the movement. Another example of magnetic-free Kalman filter was the one developed by Ligorio et al. [15]. In that case the developed filter was a linear Kalman filter applied on a single IMU placed on the hand and the reached accuracies were generally lower than 5°.The suitability of the proposed Extended Kalman Filter is further confirmed by the high Pearson's correlation coefficients achieved in the comparison with the reference signal, with values greater than 0.86 (obtained for the wrist internal-external rotation). The following limitations must be acknowledged when interpreting the present study results: a limited number of participants was considered and only the right upper limb joint angles were estimated. In addition, future efforts should be focused on the introduction of the compensation of the gyroscope bias vector in the filter state vector. In conclusion, the proposed magnetic-free Extended Kalman filter was effective in estimating the upper-limb joint angles during a traditional Yoga sequence with accuracies suitable to human movement tracking applications such as a virtual coaching solution.

ACKNOWLEDGMENT

LT's PhD scholarship was funded by TuringSense EU lab (Forlì, Italy), of which PG is the R&D VP. This work was partly funded by the Italian Ministry of University and Research under the TRAINED project (GA 2017L2RLZ2).

REFERENCES

[1] C. F. Small, J. T. Bryant, I. L. Dwosh, P. M. Griffiths, D. R. Pichora, and B. Zee, "Validation of a 3D optoelectronic motion analysis system for the wrist joint," *Clin. Biomech.*, vol. 11, no. 8, pp. 481–483, 1996.

[2] A. Filippeschi, N. Schmitz, M. Miezal, G. Bleser, E. Ruffaldi, and D. Stricker, "Survey of motion tracking methods based on inertial sensors: A focus on upper limb human motion," *Sensors*, vol. 17, no. 6, p. 1257, 2017.

[3] P. J. Figueroa, N. J. Leite, and R. M. L. Barros, "A flexible software for tracking of markers used in human motion analysis," *Comput. Methods Programs Biomed.*, vol. 72, no. 2, pp. 155–165, 2003.

[4] P. Taylor, M. C. Schall, D. Ph, and H. Chen, "Accuracy and repeatability of an inertial measurement unit system for field-based occupational studies," no. 210, pp. 1–23, 2015.

[5] P. Gui, L. Tang, and S. Mukhopadhyay, "MEMS based IMU for tilting measurement: Comparison of complementary and kalman filter based data fusion," in *2015 IEEE 10th conference on Industrial Electronics and Applications (ICIEA)*, 2015, pp. 2004–2009.

[6] A. M. Sabatini, "Quaternion-based extended Kalman filter for determining orientation by inertial and magnetic sensing," *IEEE Trans. Biomed. Eng.*, vol. 53, no. 7, pp. 1346–1356, 2006.

[7] G. Ligorio and A. M. Sabatini, "Dealing with Magnetic Disturbances in Human Motion Capture : A Survey of Techniques," 2016.

[8] S. O. H. Madgwick, "An efficient orientation filter for inertial and inertial / magnetic sensor arrays," 2010.

[9] T. Islam, M. S. Islam, M. Shajid-Ul-Mahmud, and M. Hossam-E-Haider, "Comparison of complementary and Kalman filter based data fusion for attitude heading reference system," in *AIP Conference Proceedings*, 2017, vol. 1919, no. 1, p. 20002.

[10] J. Vaganay, M.-J. Aldon, and A. Fournier, "Mobile robot attitude estimation by fusion of inertial data," in *[1993] Proceedings IEEE International Conference on Robotics and Automation*, 1993, pp. 277–282.

[11] G. Ligorio *et al.*, "A wearable magnetometer-free motion capture system: innovative solutions for real-world applications," *IEEE Sens. J.*, 2020.

[12] M. D. Shuster, "A survey of attitude representations," *Navigation*, vol. 8, no. 9, pp. 439–517, 1993.

[13] G. S. Faber, C.-C. Chang, P. Rizun, and J. T. Dennerlein, "A novel method for assessing the 3-D orientation accuracy of inertial/magnetic sensors," *J. Biomech.*, vol. 46, no. 15, pp. 2745–2751, 2013.

[14] X. Yun and E. R. Bachmann, "Design, implementation, and experimental results of a quaternion-based Kalman filter for human body motion tracking," *IEEE Trans. Robot.*, vol. 22, no. 6, pp. 1216–1227, 2006.

[15] G. Ligorio and A. M. Sabatini, "A novel Kalman filter for human motion tracking with an inertial-based dynamic inclinometer," *IEEE Trans. Biomed. Eng.*, vol. 62, no. 8, pp. 2033–2043, 2015.